Combining Differential SAR Interferometry and Copolar Phase Differences for Snow Water Equivalent Estimation

Kristina Belinska, *Graduate Student Member, IEEE*, Georg Fischer, and Irena Hajnsek, *Fellow, IEEE*

***Abstract*— The amount of water in a snow pack can be described by the snow water equivalent (SWE). SWE is a crucial parameter for hydrological models, for example, for flood predictions. Previous studies have shown that the interferometric phase between two repeat-pass synthetic aperture radar (SAR) measurements can be used to determine the change in SWE. However, a limitation of this method is phase wraps. To overcome this, the copolar phase difference (CPD) between the VV and HH channel can be used, which has been proven to be related to the depth of freshly accumulated snow. This study proposes an approach to incorporate the information on the fresh snow accumulation from the CPD into the interferometric SWE retrieval algorithm. The aim is to detect and correct interferometric phase wraps. The first results using airborne SAR data indicate that including the CPD improves the accuracy of the SWE retrieval.**

***Index Terms*— Copolar phase difference (CPD), differential interferometry, polarimetry, snow water equivalent (SWE), synthetic aperture radar (SAR).**

I. Introduction

SNOW water equivalent (SWE) refers to the amount of water in the snow pack and is required as an input parameter for hydrological models [1], for example, flood forecasting models [2]. With remote sensing, SWE measurements can be acquired on a global scale [3]. Passive microwave sensors are used to obtain large-scale SWE products but suffer from low spatial resolution [4]. In contrast, active microwave sensors such as synthetic aperture radar (SAR) offer the possibility of monitoring the Earth at a meter scale [5].

Especially, repeat pass differential interferometric SAR (DInSAR) can be used to estimate the SWE change between two acquisitions as there is a clear physical relationship between the SWE change and the DInSAR phase. Microwaves are refracted in the snow pack because the snow has different dielectric properties than air. This causes a phase delay which can be measured using the interferometric phase [6], [7].

Received 23 May 2024; revised 4 September 2024; accepted 11 September 2024. Date of publication 16 September 2024; date of current version 30 September 2024. *(Corresponding author: Kristina Belinska.)*

Kristina Belinska is with the German Aerospace Center (DLR), Microwaves and Radar Institute, 82234 Wessling, Germany, and also with the Institute of Environmental Engineering, Swiss Federal Institute of Technology in Zurich (ETH), 8093 Zürich, Switzerland (e-mail: kristina.belinska@dlr.de; belinska@ifu.baug.ethz.ch).

Georg Fischer is with the German Aerospace Center (DLR), Microwaves and Radar Institute, 82234 Wessling, Germany (e-mail: georg.fischer@dlr.de).

Irena Hajnsek is with the Institute of Environmental Engineering, Swiss Federal Institute of Technology in Zurich (ETH), 8093 Zürich, Switzerland, and also with the German Aerospace Center (DLR), Microwaves and Radar Institute, 82234 Wessling, Germany (e-mail: hajnsek@ifu.baug.ethz.ch; irena.hajnsek@dlr.de).

Digital Object Identifier 10.1109/LGRS.2024.3461229

However, the 2π ambiguity of the interferometric phase introduces phase wraps, leading to wrong SWE change estimates. These phase wraps occur when the SWE change between two acquisitions is above (or below) a certain wavelength-dependent threshold.

Applying polarimetry, the copolar phase difference (CPD) between the vertical VV and horizontal HH copolarized channels can indicate the amount of freshly fallen snow [8], [9], [10]. A physical model has been presented in [11], that uses the CPD to invert the snow depth, by assuming the density and anisotropy of a snow pack.

Since the CPD measurements can be linked to the amount of fresh snow, this study aims to include the CPD measurements in the DInSAR retrieval in order to estimate phase wraps of the interferometric phase.

In this letter, we therefore propose to combine the DInSAR SWE estimation with the polarimetric information of the radar waves to improve the performance of the retrieval.

II. Methods

A. SWE Estimation Using DInSAR

The change in SWE $\Delta \mathrm{SWE}_{\mathrm{Inf}}$ between two temporally separated SAR measurements can be retrieved using the interferometric phase $\Delta\Phi_{\mathrm{Inf}}$ between the acquisitions [6], [7]. The interferometric phase $\Delta\Phi_{\mathrm{Inf}}$ can be obtained from the complex interferometric coherence γ_{Inf}, which describes the cross correlation between the signal at the first acquisition S_1 and at the second acquisition S_2 with

$$\Delta\Phi_{\mathrm{Inf}} = \arg(\gamma_{\mathrm{Inf}}) = \arg\left(\frac{\langle S_1 S_2^* \rangle}{\sqrt{\langle S_1 S_1^* \rangle \langle S_2 S_2^* \rangle}}\right). \quad (1)$$

Radar waves are refracted in a dry snow pack due to the difference in dielectric properties between snow and air. This causes a change in the optical path length of the radar wave, which depends on the amount of snow. The relation between the SWE change $\Delta \mathrm{SWE}_{\mathrm{Inf}}$ and interferometric phase $\Delta\Phi_{\mathrm{Inf}}$ can be written as [7]

$$\Delta SWE_{\mathrm{Inf}} = \frac{\Delta\Phi_{\mathrm{Inf}}}{2k\frac{\alpha}{2}\left(1.59 + \Theta^{\frac{5}{2}}\right)}. \quad (2)$$

In this case, $k = 2\pi/\lambda$ is the wavenumber that depends on the wavelength λ. α is a parameter around 1, which is used to reduce the root mean square error (RMSE) between the exact solution and the numerical approximation. For a fixed value of $\alpha = 1$, a maximum error for incidence angles smaller than 40°

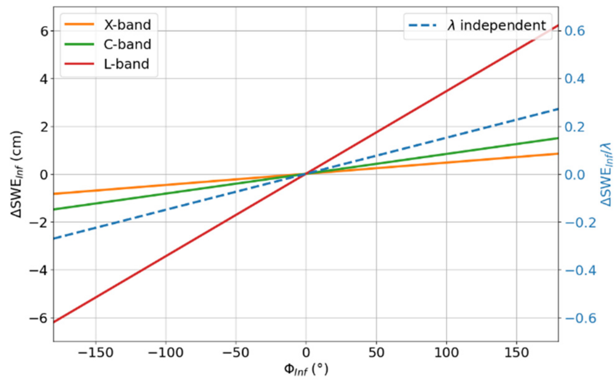

Fig. 1. SWE change $\Delta\text{SWE}_{\text{Inf}}$ in dependence on the interferometric phase for an incidence angle of 34°. The solid lines show the changes for X-, C-, and L-band. The dashed line represents the SWE change divided by the wavelength.

lies below 3%, as has been shown in [7], therefore, $\alpha = 1$ will be used. Θ is the incidence angle of the radar wave.

One limitation of this method is that the interferometric phase can only be measured in the range $[-180°, 180°]$. As a result, only $\Delta\text{SWE}_{\text{Inf}}$ in a certain interval can be estimated. Fig. 1 shows $\Delta\text{SWE}_{\text{Inf}}$ in dependence of the interferometric phase assuming an exemplary incidence angle of 34° for X-, C-, and L-band. Furthermore, the ratio between $\Delta\text{SWE}_{\text{Inf}}$ and λ is displayed to show the linear dependency independent of the wavelength. Longer wavelengths like L-band have the ability to measure higher $\Delta\text{SWE}_{\text{Inf}}$ while shorter wavelengths like the X- and C- band have a higher sensitivity to smaller changes. SWE change values exceeding the interval, as shown by the SWE change values for +/−180° interferometric phase in Fig. 1, would result in phase wraps. These phase wraps have to be corrected for an accurate $\Delta\text{SWE}_{\text{Inf}}$ estimation.

B. Link Between CPD and Snow Parameters

The CPD Φ_{CPD} can be calculated from the complex polarimetric coherence γ_{CPD} between the vertical polarized signal S_{VV} and the horizontal polarized signal S_{HH}, and can be described by the difference between the phase Φ_{VV} and Φ_{HH}

$$\Phi_{\text{CPD}} = \arg(\gamma_{\text{CPD}}) = \arg\left(\frac{\langle S_{\text{VV}} S_{\text{HH}}^* \rangle}{\sqrt{\langle S_{\text{VV}} S_{\text{HH}}^* \rangle \langle S_{\text{VV}} S_{\text{HH}}^* \rangle}}\right) = \Phi_{\text{VV}} - \Phi_{\text{HH}}. \quad (3)$$

The delay of a signal in an anisotropic snowpack depends on its polarization. The anisotropy is caused by the horizontal alignment of freshly accumulated snow grains [11]. This results in a decrease in the propagation speed of horizontally polarized radar waves, increasing the Φ_{CPD}. After a few days or weeks, the snow structure becomes more vertically oriented due to the temperature gradients that exist along the snow depth, which then can be associated with a slower propagation speed of the vertically polarized radar waves, decreasing the CPD [8].

The model proposed in [11] shows that the snow depth Z_s can be linked to the Φ_{CPD} as

$$\Phi_{\text{CPD}} = -\frac{4\pi}{\lambda} Z_s \left(\sqrt{n_V^2 - \sin^2(\Theta)} - \sqrt{n_H^2 - \sin^2(\Theta)}\right) \quad (4)$$

n_V and n_H are the refractive indices for the vertically and horizontally polarized radar waves and can be estimated by assuming a density ρ_s and anisotropy A of the snow pack [11]. For fresh snow, density values around $\rho_s = 0.2$ g/cm^3 can be measured with positive anisotropies [11].

C. Combination of DInSAR and CPD for SWE Estimation

The aim is to use (2) to estimate $\Delta\text{SWE}_{\text{Inf}}$. In the next step, polarimetric information is included to check whether phase wraps occurred. For that, the CPD change $\Delta\Phi_{\text{CPD}}$ between the two images is calculated and linked to the snow depth change ΔZ_s according to (4), with

$$\Delta Z_s = -\frac{\Delta\Phi_{\text{CPD}}}{\frac{4\pi}{\lambda}\left(\sqrt{n_V^2 - \sin^2(\Theta)} - \sqrt{n_H^2 - \sin^2(\Theta)}\right)}. \quad (5)$$

Now, ΔZ_s can be linked to the $\Delta\text{SWE}_{\text{CPD}}$ by assuming the snow density using the approximation

$$\Delta SWE_{\text{CPD}} \approx \Delta Z_s * \rho_s/\rho_{\text{water}}. \quad (6)$$

The density of water is notated with ρ_{water}.

$\Delta\text{SWE}_{\text{CPD}}$ from (6) is now used to estimate the amount of phase cycles that need to be corrected in the $\Delta\text{SWE}_{\text{Inf}}$ estimate to obtain corrected SWE change values. The applied correction criterium is:

$$|\Delta SWE_{\text{Inf}} - \Delta\text{SWE}_{\text{CPD}}| < \Delta\text{SWE}_{\text{Inf}}(\Phi = \pi). \quad (7)$$

With the criterium, we check whether adding an interferometric phase cycle reduces the difference between $\Delta\text{SWE}_{\text{Inf}}$ and $\Delta\text{SWE}_{\text{CPD}}$ and if it applies then the missing phase cycle $[\Delta\text{SWE}_{\text{Inf}}(\Phi = 2\pi)]$ is added. This step is repeated until the correction criterium is not valid anymore. This approach is more robust than translating $\Delta\text{SWE}_{\text{CPD}}$ directly into interferometric phase cycles, because it ensures that no phase wrap is added if the actual $\Delta\text{SWE}_{\text{Inf}}$ is slightly below and $\Delta\text{SWE}_{\text{CPD}}$ is slightly above the phase wrap threshold, as adding the missing phase cycles would increase the difference between the two observables.

III. Data

In March 2021, the DLR's airborne radar system F-SAR performed fully polarimetric C-band ($\lambda = 5.65$ cm) and L-band ($\lambda = 22.63$ cm) measurements over a snow-covered area in the Austrian Alps. These acquisitions were part of the SARSimHT-NG study by ESA [12]. In the time frame of the F-SAR acquisitions, snow parameters like snow depth, density, and SWE were measured by a ground team from ENVEO [13]. The first interferometric image pair is from measurements on 02.03./06.03.2021 with a small snowfall event ($\Delta\text{SWE}_{\text{Inf}} \approx 10$ mm) below the phase wrap threshold. The second interferometric pair from 06.03./19.03.2021 contains a larger snowfall event ($\Delta\text{SWE}_{\text{Inf}} \approx 70$ mm), resulting in phase wraps. To calculate $\Delta\text{SWE}_{\text{Inf}}$, the interferometric phase is calibrated with the closest corner reflector which was placed in the measured scene. Snow was removed from the corner reflectors during the measurements.

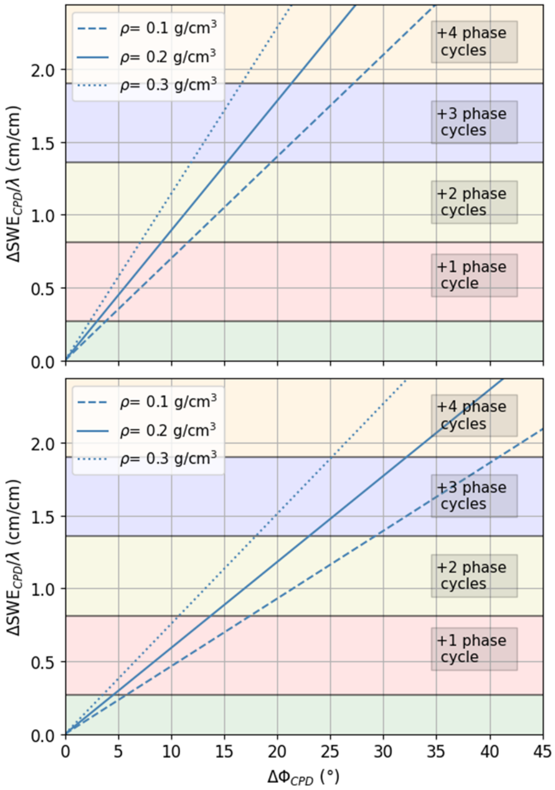

Fig. 2. Estimated SWE change $\Delta\mathrm{SWE}_{\mathrm{CPD}}/\lambda$ calculated from the CPD change for different snow densities for an incidence angle of 34°. The background colors indicate to which amount of missing phase cycles this would correspond in the DInSAR model for $\Delta\mathrm{SWE}_{\mathrm{Inf}}$. The assumed anisotropies are: (top) $A = 0.2$ (bottom) $A = 0.3$.

IV. Results

A. Sensitivity of the Model

Fig. 1 shows that in the DInSAR model, the first phase wrap for $\Theta = 34°$ occurs at $\Delta\mathrm{SWE}_{\mathrm{Inf}}/\lambda = 0.27$. This corresponds to a SWE change of $\Delta\mathrm{SWE}_{\mathrm{Inf,Wrap,C}} = 15.3$ mm at C-band and $\Delta\mathrm{SWE}_{\mathrm{Inf,Wrap,L}} = 61.1$ mm at L-Band, representing the need to correct phase wraps at small wavelengths.

When determining the $\Delta\mathrm{SWE}_{\mathrm{CPD}}$ from the polarimetric phase and comparing it to the phase wraps of $\Delta\mathrm{SWE}_{\mathrm{Inf}}$, the results in Fig. 2 are obtained. The lines mark the SWE changes for three different densities at two different anisotropies in the figures. The red area above the first horizontal line represents the region where the SWE change would be high enough to observe one wrap of the DInSAR phase. The yellow marked area corresponds to SWE changes that result in two wraps in the DInSAR phase and so forth.

Phase wraps of the CPD phase are not expected even for large SWE changes. The sensitivity of the CPD phase to SWE changes (lines in Fig. 2) is significantly lower than when using the DInSAR phase (Fig. 1). Furthermore, $\Delta\mathrm{SWE}_{\mathrm{CPD}}$ depends on density and anisotropy assumptions. Therefore, the CPD model is only used to assess the number of interferometric phase wraps and the DInSAR model is used for the actual estimation of the SWE change.

The influence of phase noise affects the SWE change estimate and can be analyzed by means of interferometric and polarimetric coherence. The estimation error for the phase can be calculated using the Cramer–Rao bounds [14]

$$\sigma_\Phi = \frac{1}{|\gamma|}\frac{\sqrt{1-|\gamma|^2}}{\sqrt{2N}}. \tag{8}$$

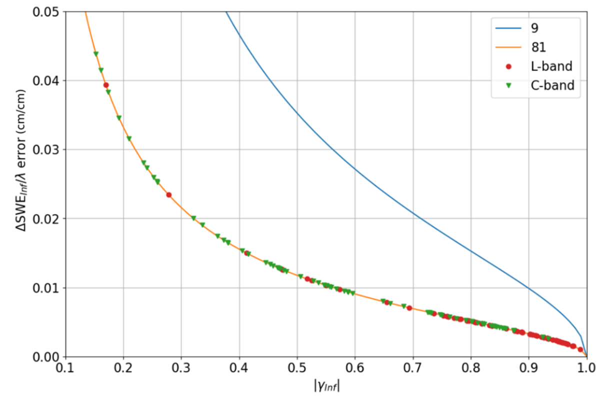

Fig. 3. Error for SWE change divided by wavelength due to phase noise in dependence of the interferometric coherence for 9 and 81 looks. The points are the C- and L-band measurements.

$|\gamma|$ is the coherence amplitude and N is the number of looks. The error can be translated into a wavelength-independent estimation error for the SWE change. For the DInSAR case, (2) is used and the results in dependence of the coherence are shown in Fig. 3. The estimation error decreases when a higher number of looks is used. For the data, a window size of 81 is used. The points correspond to F-SAR measurements at the in situ SWE locations. The L-band measurements have higher coherences, due to less temporal decorrelation, which leads to smaller $\Delta\mathrm{SWE}_{\mathrm{Inf}}$ errors relative to the wavelength.

The error due to the phase noise can be estimated also for the polarimetric case using the Cramer–Rao bounds. By propagating the phase error in (5), the following equation for the error is obtained:

$$\sigma_{\Delta Z_s} = \sqrt{\left(\frac{\partial \Delta Z_s}{\partial \Phi_{\mathrm{CPD},1}}\right)^2 \sigma^2_{\Phi_{\mathrm{CPD},1}} + \left(\frac{\partial \Delta Z_s}{\partial \Phi_{\mathrm{CPD},2}}\right)^2 \sigma^2_{\Phi_{\mathrm{CPD},2}}}. \tag{9}$$

The error $\sigma_{\Delta Z_s}$ can be translated into a SWE change error using (6). As the relative SWE change errors are higher in the polarimetric case than in the DInSAR case, the number of looks has been increased as shown in Fig. 4. It is observed that C-band has higher mean polarimetric coherence than L-band, with associated smaller $\Delta\mathrm{SWE}_{\mathrm{CPD}}$ errors in C-band.

B. Examples Using F-SAR Data

The F-SAR data can be utilized to calculate $\Delta\mathrm{SWE}_{\mathrm{Inf}}$ with (2). The comparison between the estimation results and the in situ measurements are presented in Fig. 5 (top) for both wavelengths and both polarizations. Here it has to be pointed out that interferometric coherences below 0.25 were masked out to keep the error below 10% of the phase wrap threshold, as well as incidence angles below 20° and slopes higher than 25%. Moreover, as the CPD change will be used for phase wrap corrections later, pixels with polarimetric coherence below 0.6 are also masked out so that the $\Delta\mathrm{SWE}_{\mathrm{CPD}}$ error does not exceed half of the DInSAR phase wrap threshold. It can be seen that especially for higher in situ changes, the C-band

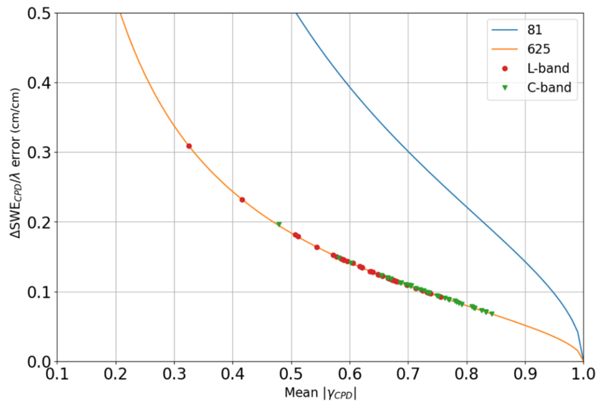

Fig. 4. Error for SWE change divided by wavelength due to phase noise in dependence of the polarimetric coherence for 81 and 625 looks for a snow density of $\rho_s = 0.1$ g/cm^3 and anisotropy of $A = 0.3$. The points are the C- and L-band measurements.

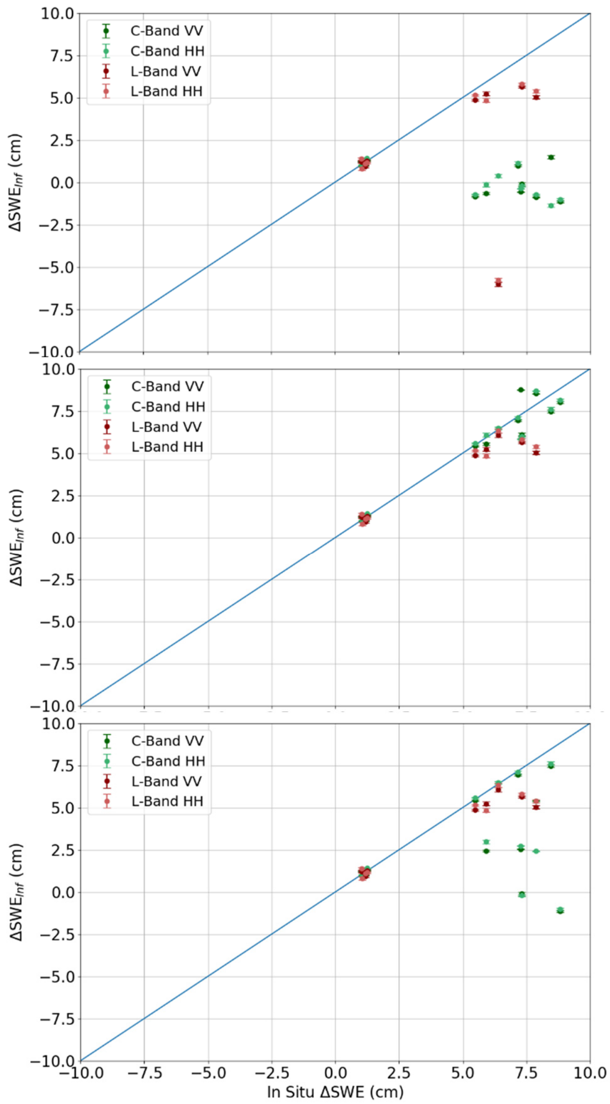

Fig. 5. Retrieved SWE values for C- and L-band in dependence of the in situ measurements. (Top) Before phase wrap correction. (Middle) After phase wrap correction based on the in situ measurements. (Bottom) After phase wrap correction based on the CPD model assuming a snow density of $\rho_s = 0.1$ g/cm^3 and anisotropy of $A = 0.2$.

estimations are clearly underestimated, indicating phase wraps due to the SWE change.

TABLE I

RMSE$_{\mathrm{REL}}$ OF THE SWE CHANGE ESTIMATES

	$RMSE_{rel}$			
Wavelength	C-band		L-band	
Polarization	VV	HH	VV	HH
No Correction	1.10	1.13	0.19	0.19
In Situ Correction	0.13	0.12	0.05	0.05
CPD Correction				
$A = 0.2$, $\rho_s = 0.1$ g/cm^3	0.72	0.72	0.05	0.05
$\rho_s = 0.2$ g/cm^3	0.74	0.72	0.05	0.05
$\rho_s = 0.3$ g/cm^3	0.72	0.71	0.14	0.15
$A = 0.3$, $\rho_s = 0.1$ g/cm^3	0.86	0.82	0.05	0.05
$\rho_s = 0.2$ g/cm^3	0.78	0.81	0.05	0.05
$\rho_s = 0.3$ g/cm^3	0.73	0.69	0.05	0.05

For validation of the phase wrap correction, in situ measurements are used to check if the actual SWE change was above the phase wrap threshold and to correct the SWE estimates accordingly. This results in Fig. 5 (middle). The C-band and L-band SWE estimates have been clearly improved with the in situ based phase wrap correction. This step shows the importance of accurate phase wrap estimations, especially for shorter wavelengths.

To test the proposed method, the CPD change between the images is calculated and used with (5) and (6) to estimate the occurrence of phase wraps. One example is shown in Fig. 5 (bottom) assuming a snow density of $\rho_s = 0.1$ g/cm^3 and anisotropy of $A = 0.2$. It can be seen that some phase wraps are correctly predicted, while some are not identified or not sufficiently corrected.

For a better comparison between the frequencies, the relative RMSE (RMSE$_{\mathrm{rel}}$) between the measurements and the retrieved SWE changes is calculated and set in relation to the wavelength with

$$\mathrm{RMSE}_{\mathrm{rel}} = \mathrm{RMSE}/\lambda. \tag{10}$$

The results of which are displayed in Table I. In general, the L-band retrieval has a smaller RMSE$_{\mathrm{rel}}$ compared to the C-band results. After performing the in situ correction, the C-band results show a higher improvement. This results from the fact that C-band estimations suffer more from phase wraps than the L-band estimations due to the shorter wavelength. Therefore, it is more likely that phase wraps in C-band have to be corrected. When performing the correction based on the CPD change, the results depend on the assumptions of snow density and anisotropy. For both wavelengths, the results improve compared to the uncorrected as some phase wraps can be reconstructed. However, the accuracy depends on the assumptions. As only the fresh snow change between the measurements is considered, assuming a small snow density and a rather high anisotropy seems appropriate. However, the preferred assumptions might depend on the snow conditions and the time span between the acquisitions.

The insufficient phase wrap detections in the CPD correction may result from the fact that snow metamorphism can occur between the acquisition dates. Due to the change in particle orientation, the measured CPD change does not solely represent the depth of fresh snow. This may improve for shorter temporal baselines.

However, the overall performance of the SWE retrieval improves compared to no correction and should be considered, when in situ data is unavailable.

V. Conclusion

The combination of DInSAR and PolSAR can help to identify and correct phase wraps of the DInSAR SWE change estimates and can therefore improve the retrieval. However, the correction has still a lower accuracy than when in situ data is used for phase wrap correction. One reason could be snow metamorphism which occurs between the measurements. Over time, the snow becomes more vertically orientated, leading to a CPD change that is not solely related to fresh snow. Another difficulty with the CPD model is that it requires assumptions on the snow density and anisotropy, which have an impact on its accuracy. However, the CPD correction improves the estimation in comparison to no correction, particularly for shorter wavelengths such as C-band. Therefore, the CPD model can contribute to efforts deriving SWE change directly from remote sensing SAR data without the need to incorporate in situ data, toward accurate large-scale measurements of SWE changes.

Acknowledgment

The authors would like to thank the DLR F-SAR team for the acquisition of the airborne SAR data and the ground team from ENVEO for the collection of in situ measurements.

References

[1] M. P. Clark et al., “Representing spatial variability of snow water equivalent in hydrologic and land-surface models: A review,” *Water Resour. Res.*, vol. 47, no. 7, pp. 1–23, Jul. 2011, doi: 10.1029/2011wr010745.

[2] T. Nester, R. Kirnbauer, J. Parajka, and G. Blöschl, “Evaluating the snow component of a flood forecasting model,” *Hydrol. Res.*, vol. 43, no. 6, pp. 762–779, May 2012, doi: 10.2166/nh.2012.041.

[3] J. Shi, C. Xiong, and L. Jiang, “Review of snow water equivalent microwave remote sensing,” *Sci. China Earth Sci.*, vol. 59, no. 4, pp. 731–745, Apr. 2016, doi: 10.1007/s11430-015-5225-0.

[4] N. Saberi, R. Kelly, M. Flemming, and Q. Li, “Review of snow water equivalent retrieval methods using spaceborne passive microwave radiometry,” *Int. J. Remote Sens.*, vol. 41, no. 3, pp. 996–1018, Feb. 2020, doi: 10.1080/01431161.2019.1654144.

[5] A. Moreira, P. Prats-Iraola, M. Younis, G. Krieger, I. Hajnsek, and K. P. Papathanassiou, “A tutorial on synthetic aperture radar,” *IEEE Geosci. Remote Sens. Mag.*, vol. 1, no. 1, pp. 6–43, Mar. 2013, doi: 10.1109/MGRS.2013.2248301.

[6] T. Guneriussen, K. A. Hogda, H. Johnsen, and I. Lauknes, “InSAR for estimation of changes in snow water equivalent of dry snow,” *IEEE Trans. Geosci. Remote Sens.*, vol. 39, no. 10, pp. 2101–2108, Oct. 2001, doi: 10.1109/36.957273.

[7] S. Leinss, A. Wiesmann, J. Lemmetyinen, and I. Hajnsek, “Snow water equivalent of dry snow measured by differential interferometry,” *IEEE J. Sel. Topics Appl. Earth Observ. Remote Sens.*, vol. 8, no. 8, pp. 3773–3790, Aug. 2015, doi: 10.1109/JSTARS.2015.2432031.

[8] S. Leinss, G. Parrella, and I. Hajnsek, “Snow height determination by polarimetric phase differences in X-band SAR data,” *IEEE J. Sel. Topics Appl. Earth Observ. Remote Sens.*, vol. 7, no. 9, pp. 3794–3810, Jun. 2014, doi: 10.1109/JSTARS.2014.2323199.

[9] A. Patil, G. Singh, and C. Rüdiger, “Retrieval of snow depth and snow water equivalent using dual polarization SAR data,” *Remote Sens.*, vol. 12, no. 7, p. 1183, Apr. 2020, doi: 10.3390/rs12071183.

[10] J. Voglimacci-Stephanopoli et al., “Potential of X-band polarimetric synthetic aperture radar co-polar phase difference for Arctic snow depth estimation,” *Cryosphere*, vol. 16, no. 6, pp. 2163–2181, Jun. 2022.

[11] S. Leinss, H. Löwe, M. Proksch, J. Lemmetyinen, A. Wiesmann, and I. Hajnsek, “Anisotropy of seasonal snow measured by polarimetric phase differences in radar time series,” *Cryosphere*, vol. 10, no. 4, pp. 1771–1797, Aug. 2016, doi: 10.5194/tc-10-1771-2016.

[12] V. Grachea, R. Horn, T. Nagler, and J. Fischer, “SARSimHT-NG—Simulation of hydroterra SAR system performance in the Mediterranean and the Alps based on experimental airborne SAR data,” DLR, Weßling, Germany, ENVEO, Innsbruck, Austria, ESA Contract 4000134680/21/NL/FF/, 2022.

[13] T. Nagler et al., “Field Campaigns on InSAR retrieval of snow mass in preparation of Copernicus ROSE-L,” presented at the Living Planet Symp., 2022.

[14] S. M. Kay, *Fundamentals of Statistical Signal Processing: Estimation Theory*. Upper Saddle River, NJ, USA: Prentice-Hall, 1993.